Functional Analysis of the *N*-Acetylglucosamine Metabolic Genes of Streptomyces coelicolor and Role in Control of Development and Antibiotic Production

Magdalena A. Swiatek, Elodie Tenconi, Sébastien Rigali and Gilles P. van Wezel

J. Bacteriol. **2012, 194(5):1136. DOI: 10.1128/JB.06370-11.**
Published Ahead of Print 22 December 2011.

JB
Journals.ASM.org

Functional Analysis of the *N*-Acetylglucosamine Metabolic Genes of *Streptomyces coelicolor* and Role in Control of Development and Antibiotic Production

Magdalena A. Świątek,[a] Elodie Tenconi,[b] Sébastien Rigali,[b] and Gilles P. van Wezel[a]

Molecular Biotechnology, Leiden Institute of Chemistry, Leiden University, Leiden, The Netherlands,[a] and Centre for Protein Engineering, Université de Liège, Institut de Chimie, Sart-Tilman, Liège, Belgium[b]

***N*-Acetylglucosamine, the monomer of chitin, is a favored carbon and nitrogen source for streptomycetes. Its intracellular catabolism requires the combined actions of the *N*-acetylglucosamine-6-phosphate (GlcNAc-6P) deacetylase NagA and the glucosamine-6-phosphate (GlcN-6P) deaminase/isomerase NagB. GlcNAc acts as a signaling molecule in the DasR-mediated nutrient sensing system, activating development and antibiotic production under poor growth conditions (famine) and blocking these processes under rich conditions (feast). In order to understand how a single nutrient can deliver opposite information according to the nutritional context, we carried out a mutational analysis of the *nag* metabolic genes *nagA*, *nagB*, and *nagK*. Here we show that the *nag* genes are part of the DasR regulon in *Streptomyces coelicolor*, which explains their transcriptional induction by GlcNAc. Most likely as the result of the intracellular accumulation of GlcN-6P, *nagB* deletion mutants fail to grow in the presence of GlcNAc. This toxicity can be alleviated by the additional deletion of *nagA*. We recently showed that in *S. coelicolor*, GlcNAc is internalized as GlcNAc-6P via the phosphoenolpyruvate-dependent sugar phosphotransferase system (PTS). Considering the relevance of GlcNAc for the control of antibiotic production, improved insight into GlcNAc metabolism in *Streptomyces* may provide new leads toward biotechnological applications.**

Streptomycetes are Gram-positive, soil-dwelling mycelial bacteria that have a complex life cycle that starts with the germination of a spore, which then grows out to form a branched mycelium of vegetative hyphae. The multicellular mycelial lifestyle of streptomycetes makes these organisms unique among bacteria, as connected compartments are formed that are separated by cross walls. When morphological differentiation is initiated, a so-called aerial mycelium is produced, and the erected aerial hyphae eventually form chains of spores (7, 13). Streptomycetes are prolific producers of natural products, producing some 50% of all known antibiotics, as well as many anticancer, antifungal, and immunosuppressant agents. The production of these so-called secondary metabolites is part of the developmental program, roughly coinciding with growth cessation and the onset of sporulation (3, 43).

As saprophytic soil bacteria, streptomycetes utilize naturally occurring polysaccharides, such as chitin, xylan, and cellulose, as carbon sources. *N*-Acetylglucosamine (GlcNAc), the monomer of chitin, is a preferred carbon and nitrogen source for streptomycetes, and the related metabolite glutamate is preferred over glucose (27, 41). Chitin is one of the most abundant polysaccharides on earth and is found, among others, in the cuticles and shells of insects and crustaceans and within the cell walls of fungi; to utilize this polysaccharide, streptomycetes have an extensive chitinolytic system (8, 37). In *Streptomyces coelicolor*, GlcNAc is a substrate for transport via the phosphoenolpyruvate-dependent phosphotransferase system (PTS) (reviewed in reference 5). During PTS-mediated carbon source uptake, a phosphoryl group is transferred from phosphoenolpyruvate to the general phosphotransferase enzyme I (EI; encoded by *ptsI*), from there to HPr (encoded by *ptsH*), and then further onto enzyme IIA ($EIIA^{Crr}$; encoded by *crr*), enzyme IIB (NagF), and, finally, enzyme IIC (NagE2) (27, 28). NagF phosphorylates the incoming GlcNAc to form *N*-acetylglucosamine-6-phosphate (GlcNAc-6P). Removal of any of the general PTS components (EI, EIIA, or HPr) blocks development (32). An alternative route for the internalization of monomeric GlcNAc exists in *Streptomyces olivaceoviridis* and probably in many other streptomycetes, namely, via the ATP-binding cassette (ABC) transporter NgcEFG, which imports both *N*-acetylglucosamine and its disaccharide, *N*,*N*′-diacetylchitobiose [$(GlcNAc)_2$], with similar affinities (47, 49). $(GlcNAc)_2$ is also imported via the ABC sugar transporter DasABC (10, 38).

We previously demonstrated that GlcNAc is an important signaling molecule for streptomycetes and a major decision point toward the onset of development and antibiotic production (32, 34). When GlcNAc accumulates under rich growth conditions (feast), it promotes growth, thereby blocking developmental processes, while under poor nutritional conditions (famine) the accumulation of GlcNAc promotes development and antibiotic production (34, 44). Under famine conditions, a complete signaling pathway was proposed, from GlcNAc uptake to the onset of antibiotic production, whereby the pleiotropic GntR family transcriptional regulator DasR controls the genes for GlcNAc transport and metabolism and for antibiotic synthesis (32, 34). Glucosamine-6-phosphate (GlcN-6P) is a key molecule in this signaling cascade and acts as an allosteric effector preventing DasR's DNA binding ability. This results in the loss of transcriptional repression of specific activator genes for antibiotic production, including *actII-*

Received 14 October 2011 **Accepted** 15 December 2011
Published ahead of print 22 December 2011
Address correspondence to Gilles P. van Wezel, g.wezel@chem.leidenuniv.nl.
Supplemental material for this article may be found at http://jb.asm.org/.

doi:10.1128/JB.06370-11

TABLE 1 Strains of *Streptomyces coelicolor* A3(2) described in this study

Strain	Genotype[a]	Reference
M145	Prototrophic SCP1$^-$ SCP2$^-$	20
GAM1	M145 *nagA*::*aacC4* Apr^r	This work
GAM2	M145 *nagB*::*aacC4* Apr^r	This work
GAM3	M145 *nagK*::*aacC4* Apr^r	This work
GAM4	M145 Δ*nagA*^{IFD}	This work
GAM5	M145 Δ*nagB*^{IFD}	This work
GAM6	M145 Δ*nagK*^{IFD}	This work
GAM7	M145 *nagKA*::*aacC4* Apr^r	This work
GAM8	M145 Δ*nagKA*^{IFD}	This work
GAM9	M145 Δ*nagB*^{IFD} *nagA*::*aacC4*	This work
GAM10	M145 Δ*nagKA*^{IFD} *nagB*::*aacC4*	This work
GAM12	GAM4/pGAM5	This work
GAM13	GAM5/pGAM6	This work

[a] IFD, in-frame deletion mutant; Apr^r, apramycin resistant.

ORF4, encoding the pathway-specific activator for actinorhodin (Act) production, and *redZ*, encoding the response regulator RedZ that activates prodiginine (Red) production. DasR also represses the *cpk* gene cluster encoding the cryptic polyketide Cpk, but this effect is probably indirect (43). Under feast conditions, the molecular mechanism for GlcNAc blocking of sporulation and antibiotic production is still unknown. Nonphosphorylation of key developmental proteins by global PTS components (EI, HPr, and EIIA^{Crr}) upon GlcNAc sensing is so far the only realistic hypothesis proposed (10, 32).

As can be gleaned from extensive studies of amino sugar metabolism in other bacteria, the signaling molecule GlcN-6P is produced from *N*-acetylglucosamine-6-phosphate by a GlcNAc-6P deacetylase (NagA) and is then converted by a GlcN-6P deaminase (NagB) to fructose-6-phosphate (Fru-6P), which enters the glycolytic pathway (1, 30, 46). To better understand the amino sugar-mediated signaling pathway in streptomycetes, dissection of GlcNAc metabolism in these organisms is required. In this work, we analyzed the GlcNAc metabolic pathway and specifically blocked one or more steps of GlcNAc utilization via directed deletion mutations. This allowed us to provide the first assessment of how the flux of GlcNAc influences the global regulatory routes that control *Streptomyces* development and antibiotic production.

MATERIALS AND METHODS

Bacterial strains and growth conditions. Bacterial strains and plasmids used in this study are listed in Table 1 and Table S1 in the supplemental material, respectively. *Escherichia coli* JM109 (36) and ET12567 (20) were used for routine cloning procedures and for extracting nonmethylated DNA, respectively. *Streptomyces coelicolor* A3(2) M145 was the parent strain for all mutants described in this work. All media and routine *Streptomyces* techniques are described in the *Streptomyces* manual of Kieser et al. (20). Cells of *E. coli* were grown in Luria-Bertani broth (LB) at 37°C. Phenotypic characterization of *Streptomyces* mutants was carried out on minimal medium (MM) and R5 agar plates (with carbon source as indicated) and in liquid NMMP or MM cultures (20) with 1% carbon sources, as indicated. Soy flour mannitol (SFM) agar plates were used to prepare spore suspensions.

Plasmids and constructs. All constructs described in this work are listed in Table S1 in the supplemental material, and oligonucleotides are listed in Table S2.

Constructs for creating gene replacement and IFD mutants. The strategy for creating knockout mutants was based on the unstable multicopy vector pWHM3 (45) as described previously (42). For deletion of *nagA*, the −1365/+6 and +1133/+2484 regions relative to the start of *nagA* were amplified by PCR, using primer pairs nagALF-1365 plus nagALR+6 and nagARF+1133 plus nagARR+2484, respectively. Fragments were cloned into pWHM3, and the engineered XbaI site was used for insertion of the *aacC4* apramycin resistance cassette flanked by *loxP* sites between the flanking regions. The presence of the *loxP* recognition sites allows the efficient removal of the apramycin resistance cassette following the introduction of plasmid pUWLcre expressing Cre recombinase (11, 19). The constructed plasmid was called pGAM1. Using essentially the same strategy as that for pGAM1, we constructed the knockout plasmids pGAM2 and pGAM3 for the single-gene replacement of *nagB* and *nagK*, respectively. pGAM2 contained the −1185/+6 and +770/+1918 regions relative to the start of *nagB*, and pGAM3 contained the −1450/+6 and +963/+2570 regions relative to the start of *nagK*. Plasmid pGAM4 for the in-frame deletion (IFD) of *nagKA* contained the upstream −1450/+6 region of *nagK* and the downstream +1133/+2484 region of *nagA*, which were amplified by PCR using primer pairs nagKLF-1450 plus nagKLR+6 and nagARF+1133 plus nagARR+2484, respectively. The *nagAB* (GAM9) double mutant was constructed by replacing *nagA* with the apramycin resistance cassette in the *nagB* IFD mutant GAM5. GAM8 was used as the parent for the *nagKAB* triple mutant GAM10, following replacement of *nagB* by the apramycin resistance cassette.

To analyze the correctness of the mutants, PCRs were done on mycelia from liquid-grown MM cultures, using oligonucleotides nagA_FOR-198 and nagA_REV+1417 for *nagA* and nagBFOR-336 and nagB_REV+1098 for *nagB*.

For complementation of the *nag* mutants, the low-copy-number vector pHJL401 (22), harboring the corresponding *nag* gene and promoter region (nucleotides [nt] −454 to +796 relative to the start of *nagB* and nt −512 to +2262 relative to the start of *nagK* were used to complement *nagK* and *nagA*), was used.

Antibiotic production. Quantification of prodiginines and actinorhodin was performed as described previously (20) and corrected for biomass (wet weight). Values were normalized against the parental strain M145 (set to 100%). Cultures were grown on R2YE agar plates overlaid with cellophane discs to allow separation of biomass and spent agar.

Production and purification of DasR. Production and purification of His$_6$-tagged DasR were based on a previously described protocol (9, 23), with several modifications. *Escherichia coli* BL21 Rosetta (DE3) cells carrying pFT240 (33) were grown at 37°C in 250 ml LB medium containing 100 μg/ml of ampicillin until the culture reached an optical density at 600 nm (OD_{600}) of 0.6. Production of His$_6$-tagged DasR was induced by addition of 1 mM isopropyl-β-D-thiogalactopyranoside (IPTG) for 3 h. Cells were collected by centrifugation and ruptured by sonication in lysis buffer (100 mM phosphate buffer, pH 8, 250 mM NaCl, 30 mM imidazole, 0.1% Triton). Soluble proteins were loaded onto a preequilibrated Ni^{2+}-nitrilotriacetic acid (NTA)-agarose column (5-ml bed volume). His$_6$-tagged DasR eluted at around 200 mM imidazole, and fractions containing the pure protein were pooled and dialyzed overnight at 4°C against electrophoretic mobility shift assay (EMSA) buffer (see below).

EMSA. EMSAs on double-stranded oligonucleotides were performed using Cy5-labeled *dre* probes (final concentration, 0.25 μM) and His$_6$-tagged DasR (final concentration, between 1.75 and 2.5 μM) in a total reaction volume of 50 μl. All reactions were carried out in EMSA buffer (10 mM Tris-Cl, pH 7.5, 1 mM dithiothreitol [DTT], 0.25 mM $CaCl_2$, 0.5 mM $MgCl_2$, 50 mM KCl, and 2% glycerol) containing a 100-fold excess of nonspecific DNA (salmon sperm DNA). After 15 min of incubation at room temperature, reaction mixtures were loaded into a 1% (wt/vol) agarose gel. Bound and unbound probes were separated by gel electrophoresis at room temperature, and fluorescent DNA was visualized using a Typhoon Trio+ variable-mode imager. Oligonucleotides (see Table S2 in the supplemental material) used to generate 40-bp double-stranded DNA probes for EMSAs were taken from the upstream regions of *dasA* (*dre*^{dasA}), *nagB* (*dre*^{nagB}), and the *nagKA* operon (*dre*^{nagKA}). The *cis*-acting

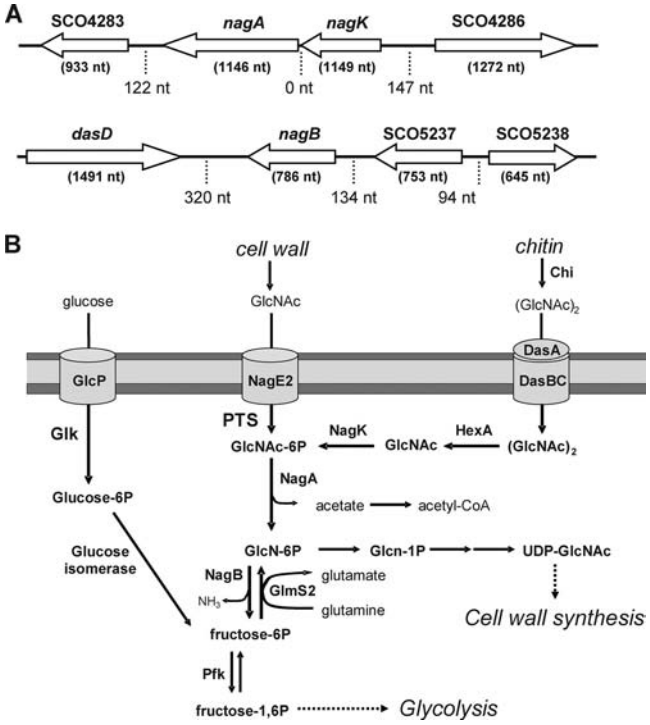

FIG 1 Genetic environment of the *nag* metabolic genes and GlcNAc-related primary metabolism. (A) Map of the genomic regions around the amino sugar utilization genes. *nagB* (SCO5236) is a single transcription unit, while *nagK* (SCO4285) and *nagA* (SCO4284) together form the *nagKA* operon. ORFs are indicated by open arrows. Lengths of the genes (in brackets below the genes) and intergenic regions (dotted lines) are indicated. (B) Amino sugar metabolism in *S. coelicolor*, with connecting pathways. Annotation is based on the KEGG database and experimental evidence. Arrows show the direction of metabolism, and the responsible enzymes are presented in bold. It is unknown whether GlcN-6P can be metabolized directly to GlcNAc-6P. Names and functions of the enzymes and the reactions they catalyze are listed in Table 2.

element OP1 of the gene for the *Bacillus licheniformis* β-lactamase repressor BlaI was used as a negative control.

RNA isolation and RT-PCR. For transcript analysis, RNA was isolated from liquid cultures of *S. coelicolor* M145 or the *dasR* mutant. Mycelium was grown in NMMP and induced by addition of 50 mM GlcNAc at an OD of ~0.2. Samples were taken before induction and 30 min after induction. RNA isolation and semiquantitative reverse transcription-PCR (RT-PCR) were carried out twice as described previously (4). Two hundred nanograms of RNA was used in each reaction mix (concentration was assessed using a Nanodrop spectrophotometer). Quantification was done using a Bio-Rad FX molecular imager with Quantity One software (Bio-Rad). Oligonucleotides used for RT-PCR are presented in Table S2 in the supplemental material.

Stereomicroscopy. Strains were grown on MM and R5 agar plates supplemented with either mannitol or GlcNAc for 5 days. The mutants were imaged using a Zeiss Lumar V12 stereomicroscope.

Computer analyses. DNA and protein data bank searches were performed using the BLAST server of the National Center for Biotechnology Information at the National Institutes of Health, Bethesda, MD (http://www.ncbi.nlm.nih.gov), as well as the *S. coelicolor* genome page services (http://strepdb.streptomyces.org.uk/). Alignments were generated with CLUSTALW, available at http://www.ebi.ac.uk/clustalw. Regulon predictions were performed using PREDetector (15). General information about the amino sugar metabolic pathway of *S. coelicolor* was found in the KEGG database (http://www.genome.jp/kegg-bin/show_pathway?sco00520).

RESULTS

***In silico* identification of GlcNAc utilization genes in *S. coelicolor*.** The genetic environment of the *nag* metabolic genes on the *S. coelicolor* chromosome and their predicted gene products are presented in Fig. 1A. The *nagK* (SCO4285) and *nagA* (SCO4284) genes have overlapping start and stop codons and encode the *N*-acetylglucosamine kinase NagK and the *N*-acetylglucosamine-6P deacetylase NagA, respectively. The NagA and NagK proteins show 34.5% and 37.2% amino acid (aa) sequence iden-

TABLE 2 Genes involved in GlcNAc transport and metabolism in *S. coelicolor* A3(2)

Gene	Locus tag	Predicted function (EC no.)	Relevant equation(s)[a]
crr	SCO1390	Global PTS component $EIIA^{Crr}$	
gdhA	SCO4683	Glutamate dehydrogenase (EC 1.4.1.4)	$Glu + H_2O + NADP^+ \Leftrightarrow 2\text{-}OG + NH_3 + NADPH + H^+$
glmM	SCO4736	Phosphoglucosamine mutase (EC 5.4.2.10)	$GlcN\text{-}1P \Leftrightarrow GlcN\text{-}6P$
glmS1	SCO4740	Glucosamine-fructose-6-phosphate aminotransferase (EC 2.6.1.16)	$Gln + Fru\text{-}6P \Leftrightarrow Glu + GlcN\text{-}6P$
glmS2	SCO2789	Glucosamine-fructose-6-phosphate aminotransferase (EC 2.6.1.16)	$Gln + Fru\text{-}6P \Leftrightarrow Glu + GlcN\text{-}6P$
glmU	SCO3122	Bifunctional *N*-acetylglucosamine-1-phosphate uridyltransferase/ glucosamine-1-phosphate acetyltransferase (EC 2.7.7.23)	$UTP + GlcNAc\text{-}1P \Leftrightarrow 2P_i + UDP\text{-}GlcNAc$ (EC 2.3.1.157), $AcCoA + GlcN\text{-}1P \Leftrightarrow CoA + GlcNAc\text{-}1P$
hexA	SCO2758	Beta-*N*-acetylglucosaminidase (EC 3.2.1.52)	$(GlcNAc)_2 + H_2O \Leftrightarrow 2\ GlcNAc$
	SCO2786	Beta-*N*-acetylhexosaminidase (EC 3.2.1.52)	$(GlcNAc)_2 + H_2O \Leftrightarrow 2\ GlcNAc$
	SCO2943	Sugar hydrolase (EC 3.2.1.52)	$(GlcNAc)_2 + H_2O \Leftrightarrow 2\ GlcNAc$
	SCO4860	Secreted hydrolase (EC 3.2.1.52)	$(GlcNAc)_2 + H_2O \Leftrightarrow 2\ GlcNAc$
nagA	SCO4284	*N*-Acetylglucosamine-6-phosphate deacetylase (EC 3.5.1.25)	$GlcNAc\text{-}6P + H_2O \Leftrightarrow GlcN\text{-}6P + OAc^-$
nagB	SCO5236	Glucosamine phosphate isomerase (EC 3.5.99.6)	$GlcN\text{-}6P + H_2O \Leftrightarrow Fru\text{-}6P + NH_3$
nagE2	SCO2907	PTS^{GlcNAc} transmembrane component EIIC	
nagF	SCO2905	PTS^{GlcNAc} transmembrane component EIIB	
nagK	SCO4285	*N*-Acetylglucosamine kinase (EC 2.7.1.59)	$GlcNAc + ATP \Leftrightarrow GlcNAc\text{-}6P + ADP$
murA	SCO2949	UDP-*N*-acetylglucosamine 1-carboxyvinyltransferase (EC 2.5.1.7)	$PEP + UDP\text{-}GlcNAc \Leftrightarrow UACCG + OP$
murA2	SCO5998	UDP-*N*-acetylglucosamine transferase (EC 2.5.1.7)	$PEP + UDP\text{-}GlcNAc \Leftrightarrow UACCG + OP$
murB	SCO4643	UDP-*N*-acetylenolpyruvoylglucosamine reductase (EC 1.1.1.158)	$UNAM + NADP^+ \Leftrightarrow UACCG + NADPH + H^+$
murQ	SCO4307	*N*-acetylmuramic acid-6-phosphate etherase (EC 4.2.-.-)	$MurNAc\text{-}6P + H_2O \Leftrightarrow GlcNAc\text{-}6P + lactate$
ptsH	SCO5841	Global PTS component HPr	
ptsI	SCO1391	Global PTS component EI	

[a] Abbreviations of metabolites: OAc^-, acetate; AcCoA, acetyl coenzyme A; $(GlcNAc)_2$, *N*,*N*′-diacetylchitobiose; $2P_i$, diphosphate; Fru, fructose; Fru-6-P, fructose-6-phosphate; GlcNAc, *N*-acetyl-D-glucosamine; GlcNAc-1P, *N*-acetylglucosamine-1-phosphate; GlcNAc-6P, *N*-acetylglucosamine-D-6-phosphate; GlcN, glucosamine; GlcN-1P, glucosamine-1-phosphate; GlcN-6P, glucosamine-6-phosphate; Gln, glutamine; Glu, glutamate; MurNAc-6P, *N*-acetylmuramic acid 6-phosphate; OP, orthophosphate; 2-OG, oxoglutarate; PEP, phosphoenolpyruvate; UDP-GlcNAc, UDP *N*-acetyl-D-glucosamine; UACCG, UDP-*N*-acetyl-3-*O*-(1-carboxyvinyl)-D-glucosamine; UNAM, UDP-*N*-acetylmuramate.

tity, respectively, to the corresponding enzymes in *E. coli*. Downstream of the *nagKA* operon lies SCO4283, encoding a phosphofructokinase-like sugar kinase, and upstream lies SCO4286, which encodes an ABC-type sugar-binding protein of unknown function. The *nagB* gene for glucosamine-6P-deaminase (SCO5236) lies immediately downstream of the *dasABCD* gene cluster involved in $(GlcNAc)_2$ uptake and degradation (10, 35) and upstream of SCO5237, encoding a likely 3-ketoacyl-(acyl carrier protein) reductase. NagB shows 44.6% amino acid sequence identity with NagB from *E. coli*. The GlcNAc-related metabolic pathway of *S. coelicolor*, based on information in the KEGG database, is shown in Fig. 1B.

Analysis of the *S. coelicolor* genome by using the BLASTP algorithm strongly suggests that there is no redundancy of the *nag* metabolic genes in *S. coelicolor*, with single *nagA*, *nagB*, and *nagK* genes. Two distant homologues of *nagA* occur in *S. coelicolor*, with gene products sharing only around 20% aa identity with NagA, namely, SCO2758, encoding a secreted β-*N*-acetylglucosaminidase most likely involved in glucan degradation (40), and SCO4860, encoding a GH20-type secreted β-*N*-acetylglucosaminidase. GH20-type hexosaminidases are involved in hydrolysis of the extracellular polysaccharide matrix in bacteria, such as β-1,6-linkages of PGA [poly-beta-(1,6)-*N*-acetylglucosamine], and do not play a role in central metabolism. The nearest functional homologue of the NagB gene is SCO2786, which encodes the endo-β-*N*-acetylhexosaminidase Hex (23% aa identity) and was shown to cleave the GlcNAc oligomers $(GlcNAc)_3$ and $(GlcNAc)_4$ in *Streptomyces plicatus* (24). Based on this *in silico* analysis, we concluded that in *S. coelicolor*, PTS-transported GlcNAc-6P is metabolized solely by the gene products of open reading frames (ORFs) SCO4284 (*nagA*) and SCO5236 (*nagB*). Similarly, we also failed to identify paralogs for the GlcNAc kinase NagK in *S. coelicolor*. In terms of the highest end-to-end aa similarity, BLASTP analysis revealed functionally unrelated enzymes, namely, a chlorohydrolase (SCO3070; 35% aa identity to NagA), a 6-phosphogluconolactonase (SCO1939; 29% aa identity to NagB), and an FGGY family carbohydrate kinase (SCO6260; 35% aa identity to NagK) with a ROK (repressors, ORFs, kinases) family signature (39).

Expression of *nagA* and *nagB* is induced by GlcNAc and repressed by DasR. Prior to assessing the effect of inactivation of the *nag* genes on the GlcNAc-mediated signaling pathway in *S. coelicolor*, we first analyzed the GlcNAc-dependent control of the *nagA*, *nagB*, and *nagK* genes. DasR is a global regulator of primary metabolism and antibiotic production and is known to control, among others, the chitinolytic system in *Streptomyces coelicolor* (9, 26), as well as *nagB* (32). There is a DasR-responsive element (*dre*) at position −68 upstream of *nagB* (tGTGGTtTAGACCAaT; dre^{nagB}) with a 13-nt match to the *dre* consensus sequence (AGT GGTCTAGACCACT; dre^{cons}) (32). Suggestively, the program PREDetector (15) also identified a *dre* element (AGaGGTCTAGt CCACT; dre^{nagKA}) at position −83 upstream of the *nagKA* operon, with 14 of 16 nt matching the *dre* consensus sequence. Furthermore, the computational prediction of the DasR regulon in five other streptomycetes revealed identical or similar *dre*-like sequences upstream of the respective *nagKA* and *nagB* orthologs, and the very high conservation suggests that these sites are true functional *cis*-acting elements. In order to validate our *in silico* predictions, EMSAs were performed *in vitro*, using His_6-tagged DasR and a short double-stranded oligonucleotide centered on

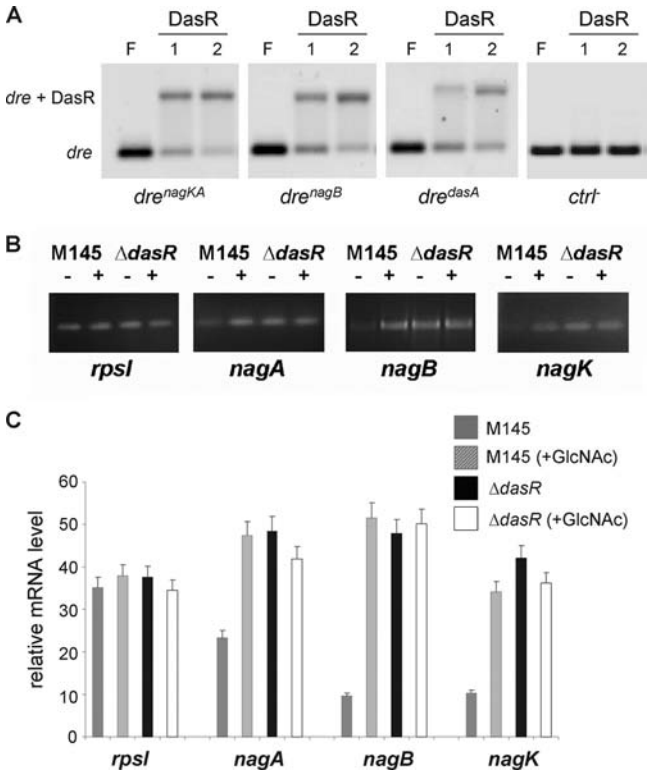

FIG 2 Direct transcriptional control of *nagKA* and *nagB* by DasR. (A) DasR binding to predicted *dre* upstream of *nagKA* and *nagB*. EMSAs were performed with pure DasR-His_6 and a 40-bp Cy5-labeled double-stranded oligonucleotide probe centered on the DasR-responsive elements (*dre*) in the promoter regions of *nagKA* (dre^{nagKA}), *nagB* (dre^{nagB}), and *dasA* (dre^{dasA}; positive control), with short flanking sequences. The *cis*-acting element of *blaI* of *Bacillus licheniformis* was used as a negative control ($ctrl^-$). Lanes: F, free probe (0.25 μM double-stranded Cy5-labeled probe); 1 and 2, DasR-*dre* binding reaction mixtures with 1.75 and 2.5 μM DasR-His_6, respectively. (B) Induction of *nag* transcription by GlcNAc and control by DasR. Semiquantitative RT-PCR was carried out on RNA isolated from the *dasR* null mutant or its parent, *S. coelicolor* M145, grown in liquid mineral medium (NMMP plus mannitol) cultures immediately prior to (−) or 30 min after (+) the addition of 25 mM GlcNAc. (C) The constitutive expression of *nagA*, *nagK*, and *nagB* in *dasR* null mutants and their enhanced transcript levels in wild-type cells 30 min after induction show that the *nag* genes are repressed by DasR and induced by *N*-acetylglucosamine.

dre^{nagKA} and dre^{nagB}. Positive specific DasR-*dre* interactions were observed for both *dre* sequences as well as for another positive control (the *dre* upstream of *dasA*), while the negative control (the *cis*-acting element of *blaI* of *Bacillus licheniformis*) was not bound by DasR (Fig. 2A).

If the *nag* genes are repressed by DasR, it would follow that their expression should be at least partially independent of induction by GlcNAc in a *dasR* null mutant. To test this hypothesis, *S. coelicolor* M145 and its Δ*dasR* null mutant were grown in liquid NMMP medium until an OD_{600} of ~0.2, followed by the addition of 25 mM GlcNAc. Mycelia were harvested for RNA preparation immediately before and 30 min after GlcNAc addition. Semiquantitative RT-PCR on total RNA samples from the wild-type strain *S. coelicolor* M145 showed induction of *nagA*, *nagK*, and *nagB* transcript levels of 2-, 3-, and 5-fold, respectively, following the addition of GlcNAc, while transcripts of the control *rspI* gene (for the ribosomal protein S9) were readily identified before and after in-

duction and did not show significant induction (Fig. 2B and C). In contrast, expression of the *nag* genes was already high in the *dasR* null mutant before induction, with similar transcript levels before and after the addition of GlcNAc (Fig. 2B and C). This is consistent with induction of the *nagA*, *nagB*, and *nagK* genes by GlcNAc and repression of these genes by DasR. The induction by GlcNAc most likely acts via the allosteric inactivation of DasR by the GlcNAc-derived metabolite GlcN-6P (32, 34).

***nagA* and *nagB* gene replacement and IFD mutants.** To study the effect of the accumulation of GlcNAc-related metabolites on growth, development, and antibiotic production, null mutants were constructed for *nagA* and *nagB*. For this purpose, we first replaced the entire coding region of *nagA* or *nagB* with the apramycin resistance cassette (*aacC4*) flanked by *loxP* sequences and then removed the cassette to generate the respective IFD mutants (see Materials and Methods). For each experiment, five transformants exhibiting the desired double-crossover phenotype (Apra^r Thio^s) were selected and verified by PCR as described in Materials and Methods. The mutants were designated GAM1 (*nagA*::*aacC4*) and GAM2 (*nagB*::*aacC4*). Following removal of the *aacC4* cassette by the Cre recombinase, IFD mutants were obtained for *nagA* (GAM4) and *nagB* (GAM5). For all experiments, both the apramycin-resistant and IFD mutants were analyzed. Considering that there were no phenotypic differences between them in terms of antibiotic production and development, from this point onwards we describe only the results obtained for the IFD mutants, unless stated otherwise. The *nagAB* double mutant GAM9 was created by replacing *nagA* with the apramycin resistance cassette in the *nagB* IFD mutant GAM5.

Effect of GlcNAc on growth of the *nagA* and *nagB* mutants in liquid-grown cultures. The addition of GlcNAc is expected to result in the accumulation of GlcNAc-6P in *nagA* mutants and GlcN-6P in *nagB* mutants (Fig. 1B). Growth of *nagB* mutants was analyzed in liquid mineral medium (NMMP) and compared to that of the parental strain *S. coelicolor* M145. While there was little difference in terms of growth on mannitol, *nagB* mutants failed to grow in the presence of GlcNAc. This is in line with the observed toxicity of the NagB substrate GlcN-6P in other bacteria (2, 29, 48). Addition of mannitol did not restore growth, strongly suggesting that rather than the inability to utilize GlcNAc, it is toxicity of a GlcNAc-derived metabolite that prevents growth of *S. coelicolor* in the absence of *nagB* (Fig. 3A). To analyze if the sensitivity to GlcNAc prevails throughout growth or occurs only during the earliest growth phases (i.e., germination and very early vegetative growth), we monitored growth in NMMP supplemented with mannitol (1% [wt/vol]), followed by the addition of 25 mM GlcNAc at an OD_{600} of 0.2 (early log phase) (Fig. 3B). Surprisingly, under these conditions, the mutant strain had a similar growth rate to that of the parent, indicating that GlcNAc toxicity is alleviated once a certain amount of biomass has accumulated. To rule out an effect specifically on spore germination, spores of *S. coelicolor* M145 and its *nagB* null mutant GAM5 were allowed to germinate for 8 h in 2× yeast extract-tryptone (2× YT) at 30°C and used as inocula for liquid mineral medium cultures. Despite the obvious emergence of germ tubes as well as many young vegetative hyphae, as assessed by phase-contrast microscopy, the germinated *nagB* mutant spores still failed to grow in the presence of GlcNAc (Fig. 3C). This illustrates that in the absence of the GlcN-6P deaminase activity of NagB, GlcNAc is toxic to young

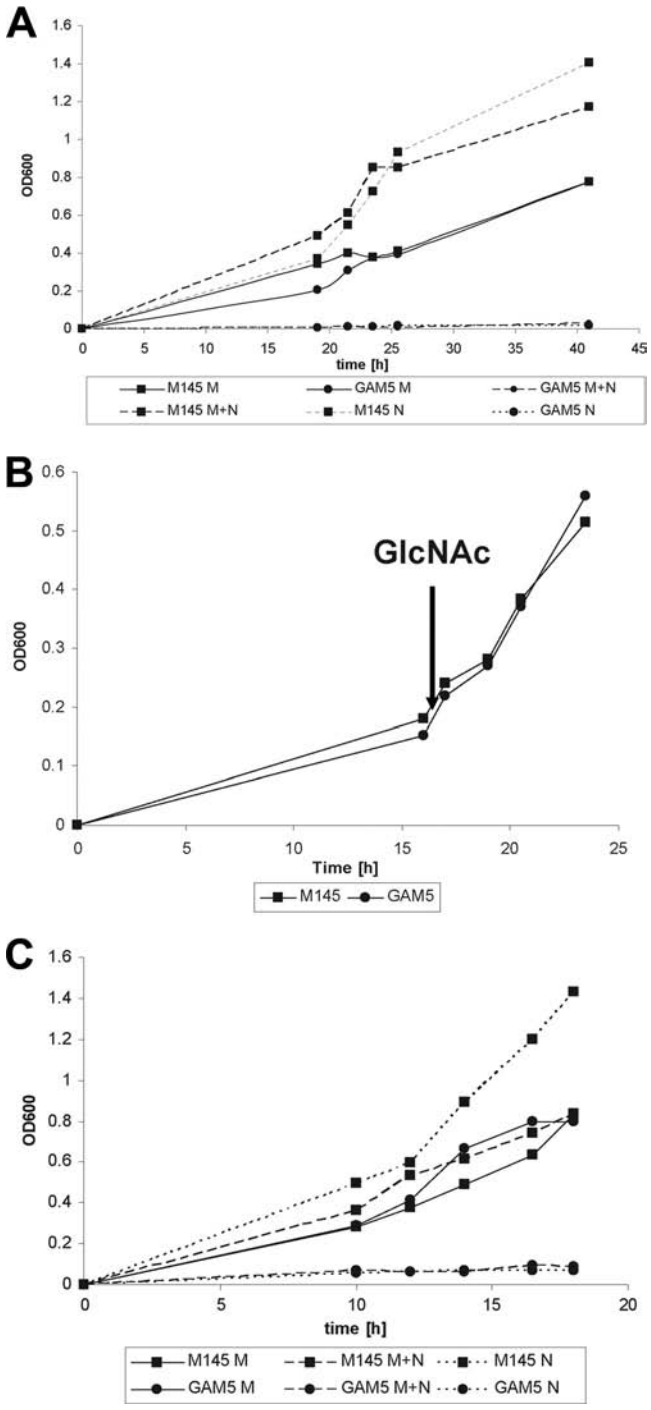

FIG 3 Effect of GlcNAc on growth of the *nagB* mutant. (A) Effects of GlcNAc on growth of *S. coelicolor* A3(2) M145 (■) and the *nagB* null mutant GAM5 (●). Strains were grown in liquid MM supplemented with either mannitol (50 mM) (M; solid lines), GlcNAc (25 mM) (N; dashed lines), or mannitol plus GlcNAc (M+N; dotted lines). (B) Effects of GlcNAc induction on growth of *S. coelicolor* A3(2) M145 (■) and the *nagB* null mutant GAM5 (●). Strains were grown in liquid NMMP supplemented with mannitol (1% [wt/vol]), followed by the addition of 25 mM GlcNAc to the cultures at an OD_{600} of ~0.2. The addition of GlcNAc is indicated with an arrow. (C) Same as panel A, but with spores that were pregerminated for 8 h in 2× YT at 30°C.

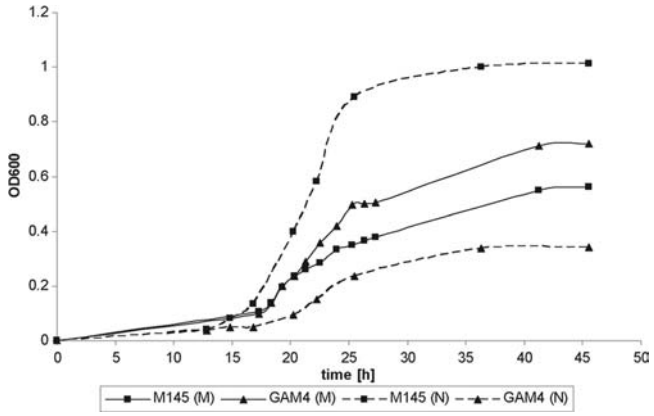

FIG 4 Effect of GlcNAc on growth of the *nagA* mutant. The effects of GlcNAc on growth of *S. coelicolor* A3(2) M145 (■) and the *nagA* null mutant GAM4 (●) are shown. Strains were grown in liquid NMMP supplemented with either mannitol (50 mM) (M; solid lines) or *N*-acetylglucosamine (25 mM) (N; dashed lines). Doubling times were derived from the linear part of the growth curves.

vegetative hyphae, but this is alleviated once a threshold amount of biomass has been produced.

The *nagA* mutant GAM4 grew with a similar doubling time (T_d; ~3 h) to that of the parent strain M145 in liquid-grown MM cultures in the presence of mannitol, but it reproducibly reached higher biomass levels (Fig. 4). Conversely, in MM with GlcNAc, the doubling time of *nagA* mutants was much longer (~5 h) than that of the parent strain M145 (~2 h). This suggests that the likely accumulation of GlcNAc-6P impairs growth of *nagA* mutants, but the effect is not as dramatic as that of the accumulation of GlcN-6P in *nagB* mutants.

Effect of GlcNAc on development and antibiotic production of *nagA* and *nagB* mutants in solid-grown cultures. The *nagA* and *nagB* mutants and the *nagAB* double mutant were similar to the parental strain in terms of colony morphology on SFM, R5, or MM agar plates supplemented with glucose, fructose, galactose, glycerol, maltose, mannitol, mannose, or xylose as the sole carbon source (see Fig. S1 in the supplemental material). However, major differences were observed when GlcNAc was added to the media. The toxicity of GlcNAc to *nagB* mutants in liquid-grown cultures was also observed on solid media, with *nagB* null mutants failing to grow on MM agar plates supplemented with 25 mM GlcNAc (Fig. 5A), while very poor growth was observed on R5 agar plates with GlcNAc (Fig. 5B). *nagA* mutants showed normal growth and development on MM agar plates with mannitol, while GlcNAc resulted in impaired growth, although some aerial hyphae were formed. Interestingly, while GlcNAc was highly toxic to *nagB* null mutants on R5 agar plates supplemented with GlcNAc, the *nagA* null mutant GAM4 was able to enter development under these conditions (Fig. 5B), a phenotype that is similar to that of mutants lacking the GlcNAc transporter gene *nagE2* (28). In line with the idea that GlcN-6P accumulation causes toxicity to *nagB* null mutants grown on GlcNAc, the double mutant GAM9 (M145 Δ*nagAB*) had a phenotype that was very similar to that of *nagA* mutants, with impaired growth on MM with GlcNAc and normal development on R5 agar plates with GlcNAc (Fig. 5). This most likely was due to the fact that the absence of *nagA* prevents the accumulation of GlcN-6P, and thus the toxicity of GlcNAc to *nagB* mutants.

The ability of the mutants to produce the pigmented antibiotics prodiginine (Red) and actinorhodin (Act) was assessed in detail on R2YE agar plates. Since Red production is switched on earlier than Act production (3), antibiotic production was measured at different time points, namely, after 42 h of growth for Red production just prior to Act biosynthesis and after 48 and 120 h for early and late Act production, respectively. Deletion of *nagA*

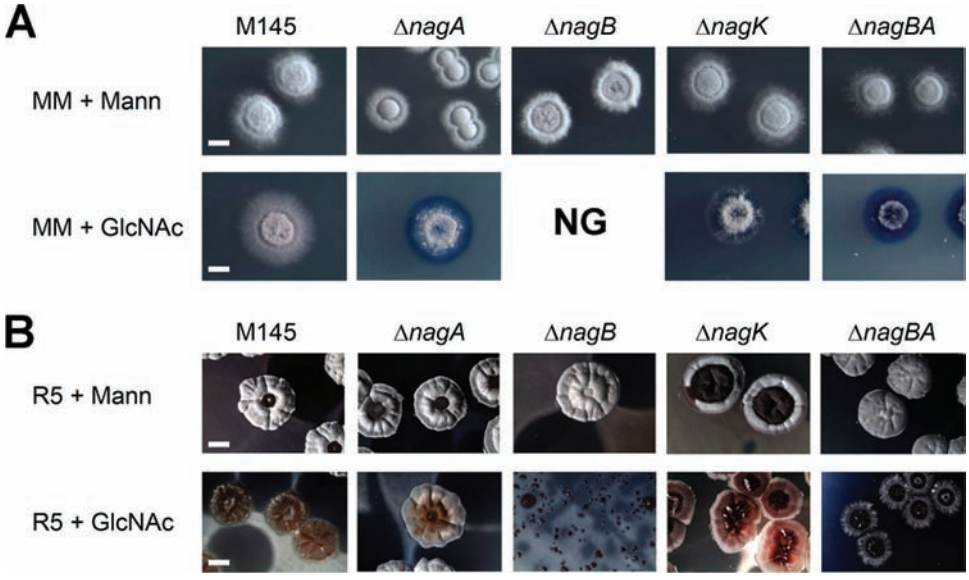

FIG 5 Phenotypic analysis of *nag* mutants. Phenotypes of *S. coelicolor* M145 and its *nagA*, *nagB*, *nagK*, and *nagAB* mutants (designated GAM4, GAM5, GAM6, and GAM9, respectively) were analyzed by stereomicroscopy. Colonies were grown for 5 days on MM (A) or R5 (B) agar plates with either mannitol (top) or GlcNAc (bottom). For phenotypes of the strains on other media, see Fig. S1 in the supplemental material. Note that *nagB* mutants failed to grow (NG) on MM supplemented with GlcNAc, while on R5 agar plates with GlcNAc, *nagB* mutants produced only a very thin layer of biomass. For complementation of the *nagA* and *nagB* mutants, see Fig. S3 in the supplemental material.

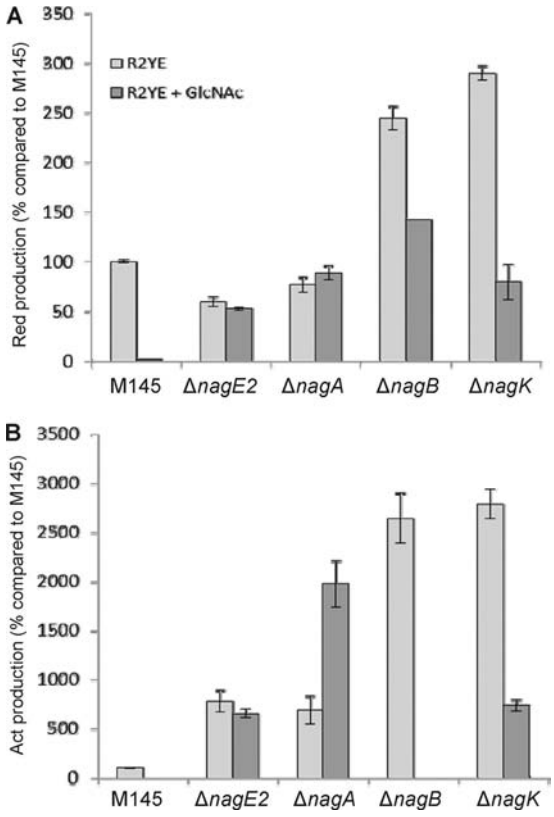

FIG 6 Quantification of antibiotic production. Production of prodiginines (top) and actinorhodin (bottom) was quantified relative to their production by the parental strain *S. coelicolor* M145 (which was set to 100%). Cultures were grown for 42 h (Red) or 48 h (Act) on R2YE agar plates with (dark bars) or without (light bars) GlcNAc. For data obtained at 120 h, see Fig. S2 in the supplemental material.

caused only a minor reduction of Red production (about 25%), while deletion of *nagB* resulted in a 2.5-fold increase of prodiginine biosynthesis (Fig. 6A). Both deletions had a more drastic effect on Act production, resulting in earlier and higher production, with 7- and 25-fold increases of Act biosynthesis after 48 h of growth for *nagA* and *nagB* mutants, respectively (Fig. 6B). After 120 h of growth, all mutants showed similar excesses of Act biosynthesis compared to the parental strain *S. coelicolor* M145 (increases of around 13-fold) (see Fig. S2 in the supplemental material). In contrast, *nagB* null mutant GAM5 formed extremely small colonies, with around 40% reduction of Red production and complete inhibition of extracellular Act production, in the presence of GlcNAc (Fig. 6). After prolonged incubation (120 h), the *nagB* null mutant GAM5 accumulated large amounts of intracellular Act on R5 agar plates supplemented with GlcNAc (see Fig. S2).

In a control experiment, the *nagA* and *nagB* gene replacement and IFD mutants were complemented with the low-copy-number vector pHJL401 (22) harboring the corresponding *nag* gene and its native promoter. *nagA* mutants GAM1 and GAM4 were complemented with pGAM5 (pHJL401/*nagKA*), and *nagB* mutants GAM2 and GAM5 were complemented with pGAM6 (pHJL401/*nagB*). The *nagKA* operon was used for complementation of *nagA* mutants to allow expression from the operon promoter. Growth on MM and R5 agar plates with and without GlcNAc demonstrated that the complemented mutants had normal growth and GlcNAc sensing, showing that the defects in growth and development in response to GlcNAc were indeed due specifically to the deletion of the respective *nag* genes (see Fig. S3 in the supplemental material). Specifically, toxicity of GlcNAc to *nagB* mutants was relieved on both media, and GlcNAc sensing was restored to both *nagA* and *nagB* mutants (e.g., bald phenotype and blocked antibiotic production on R5 agar plates with GlcNAc).

Effect of deletion of *nagK*. The sugar kinase NagK catalyzes the phosphorylation of GlcNAc to GlcNAc-6P, and the chromosomal deletion of *nagK* was performed as described for the *nagA* and *nagB* mutants (see Materials and Methods for details). We previously showed that transport of GlcNAc in *S. coelicolor* is mediated via the PTS (28). If GlcNAc is transported exclusively via the PTS, then the only internal source of GlcNAc is the dismantling of the cell wall during programmed cell death (PCD) or chitin degradation providing chitooligosaccharides [$(GlcNAc)_n$, e.g., $(GlcNAc)_2$ and $(GlcNAc)_3$] (Fig. 1B). When grown on rich medium agar plates, the *nagK* mutant presented ~27-fold-increased Red and Act production compared to the parental strain M145. Interestingly, on R2YE agar plates with GlcNAc, the *nagK* mutant showed partial loss of the GlcNAc repression effect, which we quantified to be about 75% of the wild-type GlcNAc-mediated repression. This suggests that GlcNAc may be internalized in a PTS-independent manner under these growth conditions. As expected, the additional deletion of *nagK* did not significantly alter the morphology of the *nagA*, *nagB*, or *nagAB* mutant under any of the conditions tested (data not shown).

DISCUSSION

The amino sugar *N*-acetylglucosamine (GlcNAc) is a major carbon and nitrogen source for *Streptomyces* which contributes to both cell wall synthesis and primary metabolism but also plays an important role as a developmental signaling molecule (27, 34). The signaling cascade from nutrient sensing to development and antibiotic production is a highly complex process, based on cooperative interaction between signaling molecules, the phosphorylation state of the PTS, and global and pathway-specific regulators and their effector molecules. We previously demonstrated that GlcNAc acts as a signaling molecule that controls the onset of development and antibiotic production (32, 34). Higher concentrations of GlcNAc outside the cell lock *Streptomyces coelicolor* in the vegetative growth phase under rich growth conditions (feast) but activate development and antibiotic production under poor conditions (famine). This principle has been applied successfully to enhance the expression of antibiotic biosynthetic gene clusters, including the clusters for Act, Red, and the cryptic polyketide Cpk (34). The GntR regulator DasR acts as a responsive nutrient sensor which has a pleiotropic regulon and represses, among others, *nag* metabolic genes, chitinolytic genes, and the pathway-specific activator genes for antibiotic production (9, 26, 32, 34). Since the repressing activity of DasR is relieved allosterically by the effector molecule GlcN-6P (32), it follows that controlling the flux of GlcNAc may be a promising approach for metabolic engineering relating to improved screening of novel antimicrobial compounds.

From analysis of amino sugar metabolism and connected pathways (Fig. 1B), it follows that during growth on GlcNAc, *nagA* null mutants likely accumulate GlcNAc-6P and *nagB* null mutants likely accumulate GlcN-6P. Indeed, in line with the requirement

of NagA for the production of the signaling molecule GlcN-6P, *nagA* null mutants had lost GlcNAc sensing. This underpins the current model of a direct signaling pathway from external GlcNAc to the accumulation of GlcN-6P, which then acts as an allosteric effector of the developmental regulator DasR. However, during growth on GlcNAc, *nagA* null mutants likely accumulate large amounts of GlcNAc-6P, which in *E. coli* has two important regulatory roles, namely, as an allosteric activator of NagB (6) and an effector molecule for NagC, the repressor of the *nag* regulon. In *E. coli*, inactivation of *nagA* (and hence accumulation of GlcNAc-6P) thus evokes derepression of the *nag* regulon (29, 31). An additional effect is cell lysis, suggesting a moderate toxicity of the accumulation of GlcNAc-6P in *E. coli* (48). Similar observations were made for *nagA* mutants of *Staphylococcus aureus* or *Gluconacetobacter xylinus*, which showed strongly reduced growth rates in the presence of GlcNAc (21, 50). Indeed, we also found growth reduction for *nagA* null mutants of *S. coelicolor* in liquid minimal medium with GlcNAc, and the negative effect of GlcNAc on growth of the *nagA* mutant was shown by microscopy.

The accumulation of GlcN-6P is toxic to *S. coelicolor*, as demonstrated by the inability of *nagB* mutants to grow on GlcNAc. This toxicity was relieved by the additional deletion of *nagA* or the complete *nagKA* operon (Δ*nagABK*) and could also be complemented by reintroducing *nagB* on a low-copy-number vector. Interestingly, exponentially growing cells of *nagB* mutants had overcome the sensitivity to GlcNAc, as addition of GlcNAc during early logarithmic growth (OD_{600} of ~0.2) did not lead to growth inhibition. In contrast, prolonged germination of the spores, which also resulted in the formation of many young vegetative hyphae, did not relieve the sensitivity. This strongly suggests that young vegetative hyphae in particular are sensitive to the accumulation of GlcN-6P, perhaps because alternative ways to reduce the GlcN-6P pool are not yet active enough. GlcN-6P occupies a central position between cell wall synthesis and glycolysis, and besides being converted to Fru-6P by NagB, it is also incorporated into murein following its conversion to UDP-GlcNAc by the action of GlmM (phosphoglucosamine mutase) and GlmU (*N*-acetylglucosamine-1-phosphate uridyltransferase) (Fig. 1B) (18, 25). In the absence of NagB, the major route to deplete GlcN-6P is incorporation into murein. Cell wall synthesis takes place exclusively at the apical sites (12, 14), and with very few growing tips during early growth, there may not be sufficient cell wall synthesis to convert sufficient amounts of GlcN-6P, with the net accumulation of large amounts of this toxic metabolite. An alternative explanation would be lower enzymatic activity of GlmM during early growth. In *E. coli*, GlmM is activated by phosphorylation, either by autophosphorylation or by the Ser/Thr kinase StkP (16, 17). It is still unknown how GlmM is activated in streptomycetes.

Preliminary work investigating the role of the GlcNAc kinase NagK revealed that the addition of GlcNAc has a less profound effect on development and antibiotic production in rich media when the *nagK* gene is deleted. The effect of NagK on the DasR-mediated GlcNAc nutrient sensing system suggests the accumulation of its substrate, GlcNAc. GlcNAc is internalized via the PTS in *S. coelicolor* (27, 28), but the existence of another import system that may be active under specific growth conditions cannot be ruled out. One candidate is the ABC transporter encoded by SCO6005-6007 in *S. coelicolor*, which is orthologous to the GlcNAc/chitobiose transport operon *ngcEFG* in *Streptomyces olivaceoviridis*, although the sequence similarity is low (the various gene products share 30 to 40% aa identity). Alternatively, the accumulated GlcNAc-6P (which is a labile molecule) may be hydrolyzed to GlcNAc, which is not toxic. In both cases, NagK would be required to produce GlcNAc-6P in order to allow formation of the DasR effector molecule GlcN-6P.

Interestingly, when the *nagB* null mutant was challenged with GlcNAc, we readily obtained suppressor mutants of this mutant. This is similar to observations in other bacterial systems, where spontaneous second-site mutations relieved the toxicity of accumulated sugar phosphates in *nagB* mutants (29, 48). Interestingly, when the *nagB* mutant spores were plated at a high density on MM agar plates containing GlcNAc, some colonies emerged, with a frequency of around $1:10^5$, suggesting that they had undergone spontaneous suppressor mutations to render the colonies insensitive to the toxicity of GlcNAc. Likely candidates for suppressor mutations include the GlcNAc-specific transporter genes *nagE2* and *nagF* and the metabolic genes *nagA* and *nagK*, but analysis of 16 independent suppressor mutants did not reveal changes in these genes or their promoter regions. We are currently analyzing the genomes of a series of the obtained suppressor mutants, and following recreation of the mutations in *nagB* mutants, this will reveal which genes have undergone mutations, which will shed important new light on the metabolism of GlcNAc in *Streptomyces*.

ACKNOWLEDGMENTS

We are grateful to Andriy Luzhetskyy for providing pUWLcre and for discussions and to Fritz Titgemeyer for discussions.

S.R. is a research associate of the FRS-FNRS. This work was supported by a FRIA fellowship from the FRS-FNRS to E.T. and by grant R.CFRA.1237 from the Fonds Spéciaux of the University of Liège and a VICI grant from the Netherlands Applied Research Council (STW) to G.P.V.W.

REFERENCES

1. **Alvarez-Anorve LI, Calcagno ML, Plumbridge J.** 2005. Why does *Escherichia coli* grow more slowly on glucosamine than on *N*-acetylglucosamine? Effects of enzyme levels and allosteric activation of GlcN6P deaminase (NagB) on growth rates. J. Bacteriol. **187**:2974–2982.
2. **Bernheim NJ, Dobrogosz WJ.** 1970. Amino sugar sensitivity in *Escherichia coli* mutants unable to grow on *N*-acetylglucosamine. J. Bacteriol. **101**:384–391.
3. **Bibb MJ.** 2005. Regulation of secondary metabolism in streptomycetes. Curr. Opin. Microbiol. **8**:208–215.
4. **Birko Z, et al.** 2009. Lack of A-factor production induces the expression of nutrient scavenging and stress-related proteins in *Streptomyces griseus*. Mol. Cell. Proteomics **8**:2396–2403.
5. **Bruckner R, Titgemeyer F.** 2002. Carbon catabolite repression in bacteria: choice of the carbon source and autoregulatory limitation of sugar utilization. FEMS Microbiol. Lett. **209**:141–148.
6. **Calcagno M, Campos PJ, Mulliert G, Suastegui J.** 1984. Purification, molecular and kinetic properties of glucosamine-6-phosphate isomerase (deaminase) from *Escherichia coli.* Biochim. Biophys. Acta **787**:165–173.
7. **Chater KF, Losick R.** 1997. Mycelial life style of *Streptomyces coelicolor* A3(2) and its relatives, p 149–182. *In* J. A. Shapiro and M. Dworkin (ed), Bacteria as multicellular organisms. Oxford University Press, New York, NY.
8. **Cohen-Kupiec R, Chet I.** 1998. The molecular biology of chitin digestion. Curr. Opin. Biotechnol. **9**:270–277.
9. **Colson S, et al.** 2007. Conserved cis-acting elements upstream of genes composing the chitinolytic system of streptomycetes are DasR-responsive elements. J. Mol. Microbiol. Biotechnol. **12**:60–66.
10. **Colson S, et al.** 2008. The chitobiose-binding protein, DasA, acts as a link between chitin utilization and morphogenesis in *Streptomyces coelicolor*. Microbiology **154**:373–382.
11. **Fedoryshyn M, Welle E, Bechthold A, Luzhetskyy A.** 2008. Functional

expression of the Cre recombinase in actinomycetes. Appl. Microbiol. Biotechnol. **78**:1065–1070.
12. **Flärdh K.** 2003. Growth polarity and cell division in *Streptomyces.* Curr. Opin. Microbiol. **6**:564–571.
13. **Flärdh K, Buttner MJ.** 2009. *Streptomyces* morphogenetics: dissecting differentiation in a filamentous bacterium. Nat. Rev. Microbiol. **7**:36–49.
14. **Gray DI, Gooday GW, Prosser JI.** 1990. Apical hyphal extension in *Streptomyces coelicolor* A3(2). J. Gen. Microbiol. **136**:1077–1084.
15. **Hiard S, et al.** 2007. PREDetector: a new tool to identify regulatory elements in bacterial genomes. Biochem. Biophys. Res. Commun. **357**: 861–864.
16. **Jolly L, et al.** 1999. Reaction mechanism of phosphoglucosamine mutase from *Escherichia coli.* Eur. J. Biochem. **262**:202–210.
17. **Jolly L, Pompeo F, van Heijenoort J, Fassy F, Mengin-Lecreulx D.** 2000. Autophosphorylation of phosphoglucosamine mutase from *Escherichia coli.* J. Bacteriol. **182**:1280–1285.
18. **Jolly L, et al.** 1997. The *femR315* gene from *Staphylococcus aureus*, the interruption of which results in reduced methicillin resistance, encodes a phosphoglucosamine mutase. J. Bacteriol. **179**:5321–5325.
19. **Khodakaramian G, et al.** 2006. Expression of Cre recombinase during transient phage infection permits efficient marker removal in *Streptomyces.* Nucleic Acids Res. **34**:e20.
20. **Kieser T, Bibb MJ, Buttner MJ, Chater KF, Hopwood DA.** 2000. Practical *Streptomyces* genetics. The John Innes Foundation, Norwich, United Kingdom.
21. **Komatsuzawa H, et al.** 2004. The gate controlling cell wall synthesis in *Staphylococcus aureus.* Mol. Microbiol. **53**:1221–1231.
22. **Larson JL, Hershberger CL.** 1986. The minimal replicon of a streptomycete plasmid produces an ultrahigh level of plasmid DNA. Plasmid **15**: 199–209.
23. **Mahr K, et al.** 2000. Glucose kinase of Streptomyces coelicolor A3(2): large-scale purification and biochemical analysis. Antonie Van Leeuwenhoek **78**:253–261.
24. **Mark BL, et al.** 1998. Structural and functional characterization of Streptomyces plicatus beta-*N*-acetylhexosaminidase by comparative molecular modeling and site-directed mutagenesis. J. Biol. Chem. **273**:19618–19624.
25. **Mengin-Lecreulx D, van Heijenoort J.** 1994. Copurification of glucosamine-1-phosphate acetyltransferase and *N*-acetylglucosamine-1-phosphate uridyltransferase activities of *Escherichia coli*: characterization of the *glmU* gene product as a bifunctional enzyme catalyzing two subsequent steps in the pathway for UDP-*N*-acetylglucosamine synthesis. J. Bacteriol. **176**:5788–5795.
26. **Nazari B, et al.** 2011. High expression levels of chitinase genes in *Streptomyces coelicolor* A3(2) grown in soil. FEMS Microbiol. Ecol. **77**:623–635.
27. **Nothaft H, et al.** 2003. The phosphotransferase system of *Streptomyces coelicolor* is biased for *N*-acetylglucosamine metabolism. J. Bacteriol. **185**: 7019–7023.
28. **Nothaft H, et al.** 2010. The permease gene *nagE2* is the key to *N*-acetylglucosamine sensing and utilization in *Streptomyces coelicolor* and is subject to multi-level control. Mol. Microbiol. **75**:1133–1144.
29. **Plumbridge J.** 2009. An alternative route for recycling of *N*-acetylglucosamine from peptidoglycan involves the *N*-acetylglucosamine phosphotransferase system in *Escherichia coli.* J. Bacteriol. **191**:5641–5647.
30. **Plumbridge J, Vimr E.** 1999. Convergent pathways for utilization of the amino sugars *N*-acetylglucosamine, *N*-acetylmannosamine, and *N*-acetylneuraminic acid by *Escherichia coli.* J. Bacteriol. **181**:47–54.
31. **Plumbridge JA.** 1991. Repression and induction of the *nag* regulon of *Escherichia coli* K-12: the roles of *nagC* and *nagA* in maintenance of the uninduced state. Mol. Microbiol. **5**:2053–2062.
32. **Rigali S, et al.** 2006. The sugar phosphotransferase system of *Streptomyces coelicolor* is regulated by the GntR-family regulator DasR and links *N*-acetylglucosamine metabolism to the control of development. Mol. Microbiol. **61**:1237–1251.
33. **Rigali S, et al.** 2004. Extending the classification of bacterial transcription factors beyond the helix-turn-helix motif as an alternative approach to discover new cis/trans relationships. Nucleic Acids Res. **32**:3418–3426.
34. **Rigali S, et al.** 2008. Feast or famine: the global regulator DasR links nutrient stress to antibiotic production by *Streptomyces.* EMBO Rep. **9**:670–675.
35. **Saito A, et al.** 2007. The *dasABC* gene cluster, adjacent to *dasR*, encodes a novel ABC transporter for the uptake of *N,N′*-diacetylchitobiose in *Streptomyces coelicolor* A3(2). Appl. Environ. Microbiol. **73**:3000–3008.
36. **Sambrook J, Fritsch EF, Maniatis T.** 1989. Molecular cloning: a laboratory manual, 2nd ed. Cold Spring Harbor Laboratory Press, Cold Spring Harbor, NY.
37. **Schrempf H.** 2001. Recognition and degradation of chitin by streptomycetes. Antonie Van Leeuwenhoek **79**:285–289.
38. **Seo JW, Ohnishi Y, Hirata A, Horinouchi S.** 2002. ATP-binding cassette transport system involved in regulation of morphological differentiation in response to glucose in *Streptomyces griseus*. J. Bacteriol. **184**:91–103.
39. **Titgemeyer F, Reizer J, Reizer A, Saier MH, Jr.** 1994. Evolutionary relationships between sugar kinases and transcriptional repressors in bacteria. Microbiology **140**:2349–2354.
40. **Tsujibo H, et al.** 1998. Cloning, characterization and expression of beta-*N*-acetylglucosaminidase gene from *Streptomyces thermoviolaceus* OPC-520(1). Biochim. Biophys. Acta **1425**:437–440.
41. **van Wezel GP, et al.** 2006. Unlocking *Streptomyces* spp. for use as sustainable industrial production platforms by morphological engineering. Appl. Environ. Microbiol. **72**:5283–5288.
42. **van Wezel GP, et al.** 2005. GlcP constitutes the major glucose uptake system of *Streptomyces coelicolor* A3(2). Mol. Microbiol. **55**:624–636.
43. **van Wezel GP, McDowall KJ.** 2011. The regulation of the secondary metabolism of *Streptomyces*: new links and experimental advances. Nat. Prod. Rep. **28**:1311–1333.
44. **van Wezel GP, McKenzie NL, Nodwell JR.** 2009. Applying the genetics of secondary metabolism in model actinomycetes to the discovery of new antibiotics. Methods Enzymol. **458**:117–141.
45. **Vara J, Lewandowska-Skarbek M, Wang YG, Donadio S, Hutchinson CR.** 1989. Cloning of genes governing the deoxysugar portion of the erythromycin biosynthesis pathway in *Saccharopolyspora erythraea* (*Streptomyces erythreus*). J. Bacteriol. **171**:5872–5881.
46. **Vogler AP, Lengeler JW.** 1989. Analysis of the *nag* regulon from *Escherichia coli* K12 and *Klebsiella pneumoniae* and of its regulation. Mol. Gen. Genet. **219**:97–105.
47. **Wang F, Xiao X, Saito A, Schrempf H.** 2002. *Streptomyces olivaceoviridis* possesses a phosphotransferase system that mediates specific, phosphoenolpyruvate-dependent uptake of *N*-acetylglucosamine. Mol. Genet. Genomics **268**:344–351.
48. **White RJ.** 1968. Control of amino sugar metabolism in *Escherichia coli* and isolation of mutants unable to degrade amino sugars. Biochem. J. **106**:847–858.
49. **Xiao X, et al.** 2002. The novel *Streptomyces olivaceoviridis* ABC transporter Ngc mediates uptake of *N*-acetylglucosamine and *N,N′*-diacetylchitobiose. Mol. Genet. Genomics **267**:429–439.
50. **Yadav V, et al.** 2011. *N*-Acetylglucosamine 6-phosphate deacetylase (NagA) is required for *N*-acetylglucosamine assimilation in *Gluconacetobacter xylinus*. PLoS One **6**:e18099.